Tr. J. of Engineering and Environmental Science
22 (1998) , 245 – 254.

The Computational Simulation of the Concentration Field of a Condensing Water Vapour Jet and Comparison with Experimental Data

Şenol BAŞKAYA
Gazi University, Faculty of Engineering and Architecture,
Department of Mechanical Engineering
06570, Maltepe, Ankara-TURKEY

Received 19.06.1997

Abstract

Concentration fields of water vapour, water droplet and air are presented from numerical simulation results of a turbulent water vapour jet discharged into ambient air, resulting in a two-phase (liquid and vapour), two-fluid (air and water) condensing free jet. Calculations were made with a computational fluid dynamics (CFD) code. Axial and radial concentration values from CFD simulations, are reported and compared with experimental measurements using an isokinetic sampling probe. Centreline decay rates were calculated for this condensing jet and compared with data from the literature. CFD results were very close to experimental measurements, and condensation effects on concentration distributions were found to be negligible. In the design and operation of industrial plants it is necessary to ensure the safety of the plant against possible effects caused by various types of jet flow arising from pipe breaks. The present results will be helpful in predicting the environmental effects of such jets.

Key Words: Fluid Jet, Two-Phase Flow, Computational Fluid Dynamics (CFD), Condensation, Concentration.

Yoğuşan bir Su Buharı Jetinin Konsantrasyon Dağılımının Sayısal Simülasyonu ve Deneysel Verilerle Karşılaştırılması

Özet

Yoğuşan çift fazlı (sıvı ve gaz), çift akışkanlı (hava ve su) bir serbest jet haline dönüşen, hava ortamına verilen türbülanslı su buharı jetinin su buharı, su damlacıkları ve hava konsantrasyon dağılımları sayısal simülasyon sonuçlarından sunulmuştur. Hesaplamalar bir sayısal akışkanlar dinamiği (SAD) kodu kullanılarak gerçekleştirildi. SAD simülasyonlarından elde edilen eksenel ve radyal konsantrasyon değerleri sunulmuş ve izokinetik örnekleme probu kullanılarak elde edilen deneysel değerlerle karşılaştırılmıştır. Bu yoğuşan jet için eksenel dağılım değerleri hesaplanmış ve literatürde bulunan sonuçlarla karşılaştırılmıştır. SAD sonuçları deneysel ölçümlere çok yakın ve yoğuşmanın konsantrasyon dağılımları üzerine etkisi ihmal edilebilecek seviyede bulunmuştur. Endüstriyel tesislerin tasarımında ve işletilmesinde tesisin boru çatlamalarından kaynaklanan değişik tipdeki jet akışlarının sebeb olabileceği etkilere karşı güvenliğinin sağlanması şarttır. Bu araştırma sonuçları söz konusu jetlerin çevresel etkilerinin tahmininde yardımcı olacaktır.

Anahtar Sözcükler: Akışkan Jeti, Çift Fazlı Akış, Sayısal Akışkanlar Dinamiği (SAD), Yoğuşma, Konsantrasyon.

1. Introduction

In addition to numerous industrial applications (e.g. high pressure, high temperature steam pipe breaks), jet flows in which the density varies due to exchanges of heat and/or mass are also important from a fundamental viewpoint. The mixing behaviour of various jet flows has been the subject of a great deal of research. Any number of text books can be consulted for discussions and theoretical background (see e.g. Abramovich 1963, Rajaratnam 1976, Chen and Rodi 1980 for reviews). However, mixing characteristics like concentration fields and entrainment rates have been reported mostly for non-condensing gas jets such as air-to-air jets and other ideal gas jets.

In the literature, the self-preserving behaviour of constant-density jets in the fully developed region is generally accepted. Several investigations have been made on variable density jets to show similar self-preserving states in the fully developed flow region. Global density ratio (R_ρ) effects on the self-preservation behaviour of axisymmetric turbulent jets have been investigated by Pitts (1991) and Richards and Pitts (1993). Pitts (1991) used Rayleigh light scattering to determine time averaged concentration along the centreline of jets with different properties in the fully developed region of the jet. Density ratios of 0.14 to 5.11 were used. They reported that the behaviour of axisymmetric turbulent jets of different global density ratios were predicted well by a similarity analysis appropriate for constant density jets. They also reported that the position of the virtual origin was strongly dependant on the global density ratio. This work was extended by Richards and Pitts (1993) who studied the effects of initial conditions with initial density differences imposed by using helium, methane and propane. They tested the hypothesis that all axisymmetric turbulent free jets become asymptotically independent of the source conditions and may be described by classical similarity analysis. By referring to previous findings concerning variable density jet investigations, they concluded that there were exist conflicting results regarding the achievement of an asymptotic state by variable density jets. However, from their own experimental study they state very clearly that in the fully developed region axisymmetric turbulent free jets decay at the same rate, spread at the same half-angle, and both the mean and r.m.s. mass fraction values collapse in a form consistent with full self-preservation, regardless of the initial conditions.

A wide variety of papers can be found on the effects of density variations on the structure of low-speed turbulent flows, which was the focus of the Euromech 237 Colloquium (Marseille 1988). For instance, Green and Whitelaw (1988) used a combination of laser-Doppler anemometry, laser-Rayleigh scattering and hot-wire anemometry to determine the velocity and concentration characteristics of Freon-12, helium and air jets into still air. The reader is referred to the proceedings of this colloquium for more details. The concentration field of turbulent jets has also been reported by many other researchers. Results from the present study are compared with the data reported by Hinze and van der Hegge Zijnen (1949), Becker et al. (1967), Birch et al. (1978), Grandmaison et al. (1982) Pitts (1991a), Richards and Pitts (1993) and Başkaya et al. (1998).

Condensing jets have not attracted as much attention as non-condensing jets. Several Soviet researchers have made investigations into condensing jets. Most of this work was published in Russian. However, there are a few translations available which compile most of these studies. Vatazhin et al. (1984) investigated turbulent jets in the presence of condensation consisting of a gaseous phase (air and water vapour) and a condensed disperse phase (water droplets). They analyzed the possibility of controlling the condensation process by introducing foreign particles into the flow. They made axial temperature measurements using a Chromel-Alumel thermocouple, under varying initial jet temperatures. They compared these profiles with those calculated for the case of a non-condensing jet to show the sharp transition into the condensation region. In a later study, Vatazhin et al. (1985) performed the same measurements on jets with a greater variation of discharge and ambient conditions. Strum and Toor (1992) examined condensing turbulent fog jets generated by issuing saturated water vapour-air mixtures at 63 and 85°C into a room at ambient temperature and relative humidity. Temperature increase due to condensation in the region of fog formation, the spatial distribution of the maximum condensation driving force, and the observed increase in temperature fluctuations in the fog jet over a dry jet are the three aspects they focused on.

The results presented in this paper are part of a much more comprehensive study on steam jets with different properties operated under various conditions as reported by Başkaya et al. (1995, 1997, 1998). However, the CFD simulations were con-

centrated only on one case. The properties of the simulated jet were as follows: supply pressure P_0=143kPa, supply temperature T_0=110°C, nozzle exit to ambient density ratio ρ_e/ρ_{amb}=0.53, Reynolds number $Re_D = 2.3 \times 10^5$ and steam supply mass flow rate m=23.21 g/s.

2. Experimental Apparatus

The main part of the experimental rig consisted of a saturated steam supply, a 15 kW superheater, a servo valve and pressure gauge for controlling the supply pressure, a smoothly contoured contraction nozzle (according to BS1042) with a 12mm exit diameter, an orifice plate (according to BS1042) with a differential pressure transducer for mass flow rate measurements, an extraction fan and ducting for the removal of discharged steam from experimental enclosure and finally an isokinetic sampling probe and collection apparatus. A special purpose isokinetic sampling probe was designed and manufactured. Further details are given by Başkaya et al. (1995, 1998). A schematic drawing of the steam jet and the nozzle is given in Fig. 1 with various definitions necessary for the analysis undertaken.

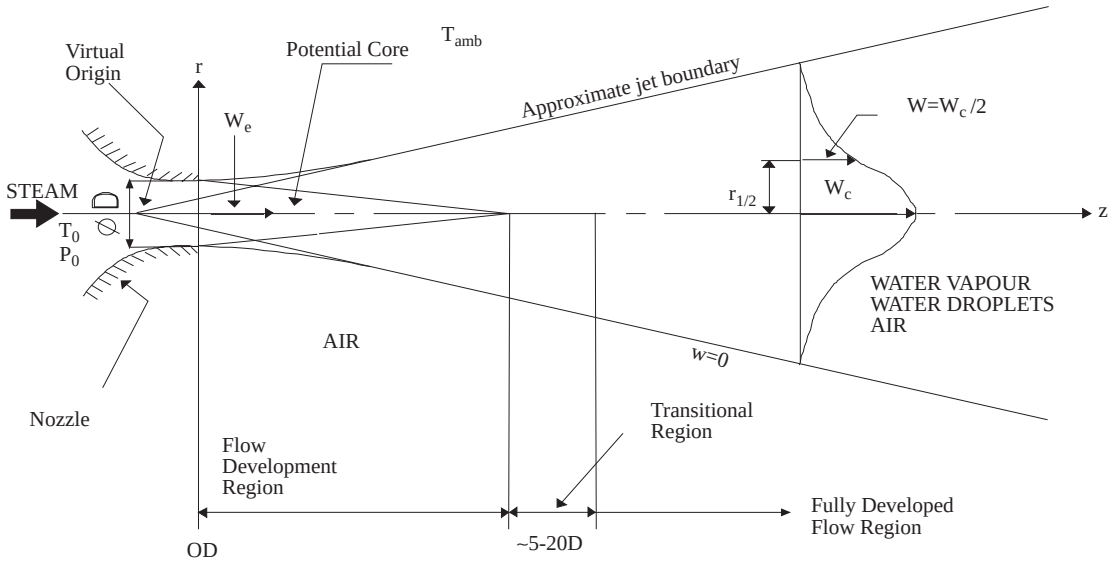

Figure 1. Schematic drawing of nozzle and steam jet flow field with definitions.

3. Theoretical Basis

The water vapour (steam) jet investigated discharges into the atmosphere as a one-component, single-phase fluid (steam). However, the flow goes through a phase-change and mixes with another one-component, single-phase fluid (air) and hence, it has different constituents at different locations (e.g. just steam in the core region). Mass fractions of the components of the jet vary throughout the jet. In the present simulations the steam jet and necessary boundary conditions were chosen in a simplified form. It was assumed that the steam leaving the nozzle was wet with inlet boundary conditions calculated from wet-equilibrium expansion. Phase changes were ignored in the mixing of the wet steam with the surrounding air. Hence, the theoretical approach taken to solve the steam jet flow was based upon the assumption that the steam-droplet-air mixture is locally homogeneous (mechanical and thermodynamic equilibrium). The resulting governing equations were solved using the commercial CFD code PHOENICS.

3.1. Mixture Properties

At any location in the jet, the air, water vapour and water droplet parts of the jet were assumed to be fully dispersed in each other and have a common velocity. All components were assumed to have a common pressure and temperature, with different partial conditions. The static pressure, stagnation temperature, velocities and mass fractions were solved in PHOENICS using the governing equations. How-

ever, properties such as density, specific heat and specific gas constant were calculated using additional user-generated coding sequences which were introduced into PHOENICS by the author. This was done according to the values for the mass fractions in order for the flow to be treated as though it were a single phase flow. The equations for the mixture properties specific heat c_{pmix}, specific gas constant R_{mix} and density ρ_{mix} are given below.

$$c_{p_{mix}} = \alpha c_{p_{air}} + \beta c_{p_{vap}} + \omega c_{p_{drop}} \quad (1)$$

$$R_{mix} = \alpha R_{air} + (\beta + \omega) R_{H_2O} \quad (2)$$

$$\rho_{mix} = \frac{P_{tot}}{R_{mix} T} \quad (3)$$

where the air (α), water vapour (β) and water droplet (ω) mass fractions are defined as:

$$\alpha = \frac{m_{air}}{m_{mix}}, \beta = \frac{m_{vap}}{m_{mix}}, \omega = \frac{m_{drop}}{m_{mix}}$$

$$\alpha + \beta + \omega = 1 \quad (4)$$

In the above equations 'air' denotes air, 'vap' denotes water vapour, 'drop' denotes water droplets, 'H_2O' the total water content and 'm' is the mass flow rate. By taking into account the properties of the simulated jet in terms of pressure and temperature variations throughout the solution domain, an assumption of constant properties was made for the jet components as follows: c_{pair} =1005 J/kg K, c_{pvap} =1900 J/kg K, c_{pdrop} =4200 J/kg K, R_{air} =287.1 J/kg K and R_{H_2O}=461.5 J/kg K.

4. Numerical Procedure

Details about the PHOENICS code are well documented in the literature. PHOENICS has been used for many jet simulations, see e.g. Malin (1988) and Adair et al. (1992). These publications should be consulted for numerical algorithms and other general procedures.

In the present study interpolations were made using the upwind-interpolation scheme together with slabwise iteration cycles in the main flow direction (z-coordinate). A conventional staggered-grid arrangement was employed for the discretization of the momentum equations (Patankar, 1980). The overall procedure has been described in detail by Spalding (1991). The simulations were made with an elliptic solver. The computations were for two-dimensions (axial [z] and transverse [r]) using polar coordinates and an axis of symmetry. Fig. 2 shows the grid distribution in the r-z plane. The number of cells is 50 in both coordinate directions. The physical size in the z-direction is 756mm (L), and in the r-coordinate it is 206mm.

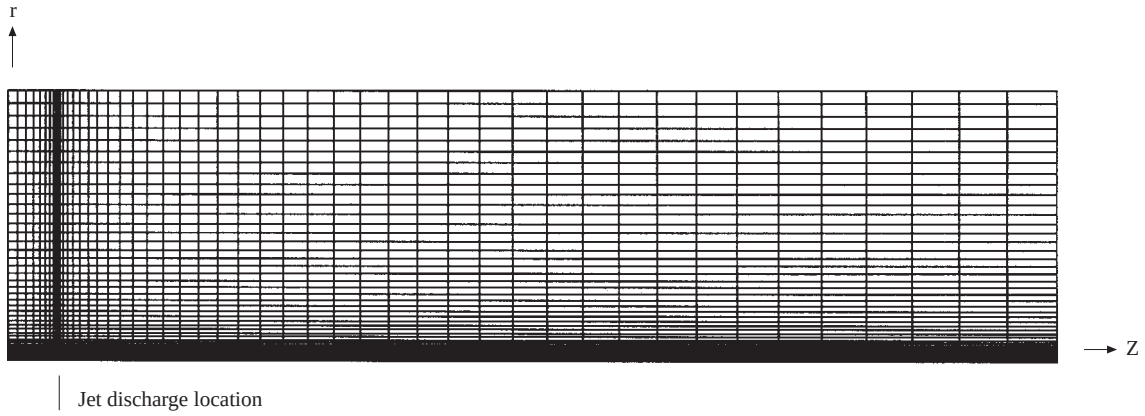

Figure 2 Grid structure of the computational domain.

Very fine grids were used near the nozzle exit and the jet centreline by applying grid power options. The grid dependence was checked (see Fig. 3a), and the solutions were obtained for 50x50 cells. False time step relaxation was used for all the solved variables except pressure, for which linear relaxation was used to obtain more rapid convergence (Patankar 1980, Spalding 1991).

The boundary conditions of the simulated steam jet were as follows. At the centreline (r=0):

$$\frac{\partial w}{\partial r} = 0, \frac{\partial T}{\partial r} = 0, \frac{\partial m}{\partial r} = 0, \quad (5)$$

for all values of z. Here w is the axial velocity, T the temperature and m is the mass flow rate. At the edge of the mixing region (r = ∞):

$$lim_{r\to\infty} w(z,r) = 0, lim_{r\to\infty} T(z,r) = T_{amb}, \\ lim_{r\to\infty} m(z,r) = m_{air}, lim_{r\to\infty} P(z,r) = P_{amb} \quad (6)$$

At the nozzle exit from experimental conditions (z = 0, r < D/2):

$$m = m_{vap} + m_{drop}, T = T_0, w = w_e \quad (7)$$

At the far end of the solution domain (z=L):

$$lim_{z\to\infty} T(z,r) = T_{amb}, lim_{z\to\infty} m(z,r) = m_{air}, \\ lim_{z\to\infty} P(z,r) = P_{amb} \quad (8)$$

The key assumptions/simplifications were that the mixture is dilute and the molecular diffusivity is negligible compared with the turbulent diffusivity. The diffusivities for heat, water vapour, water droplets and air are identical. This assumption of equal diffusivities is equivalent to saying that their rates of spread are identical, or that the turbulent Lewis number is 1.0. Another key assumption was that the velocities of all constituents of the jet medium are equal. These assumptions have been made, confirmed and applied by many researchers in the literature, see e.g. Strum and Toor (1992), Vatazhin et al. (1985).

At the inlet the mass input was specified using the jet velocity and density corresponding to values obtained from experimental measurements. Mass fractions for water vapour and water droplets were defined as the steam inlet boundary condition, obtained from wet equilibrium expansion calculations for the nozzle. For the energy equation the stagnation temperature of the jet was defined. The Reynolds number was specified for the calculation of the laminar kinematic viscosity as

$$Re_D = \frac{\rho_e w_e D}{\mu_e} \quad (9)$$

where the density ρ_e, the viscosity μ_e, and the velocity w_e are all values for the nozzle exit and D is the nozzle exit diameter. The k-ε turbulence model was used, where the inlet turbulence kinetic energy was estimated using

$$k = 0.0001(w_e)^2 \quad (10)$$

The inlet dissipation rate was estimated using

$$\varepsilon = 0.1643k^{1.5}/L_c \quad (11)$$

where L_c is the characteristic length at the inlet estimated from

$$L_c = 0.035D \quad (12)$$

5. Simulation Results

Grid dependency checks of the simulation results and the check of dependence of convergence on the number of sweeps used in the solution procedure are important before attempting a final solution. Fig. 3a shows the dependence of the centreline decay of temperature on the number of cells used in the computational domain. The 30×30 solutions are insufficient as there is an obvious difference between them and the other solutions, especially in the prediction of the core length. The differences between the 50×50 and 70×70 cell number solutions are very small and hence using 50×50 cells was considered to be sufficient for a grid independent solution.

The number of sweeps needed for a fully converged solution was checked as illustrated in Fig. 3b. After 500 sweeps the values obtained do not change with increasing number of sweeps. Thus, the final solutions were obtained with 50×50 cells and 500 sweeps.

The computational results of the radial distribution of air, water vapour and water droplet mass fractions are shown next. Dimensional radial distributions of air mass fraction are given in Fig. 4a for z/D=3 to 50 and in Fig. 4b for z/D=20 to 50.

Radial water vapour mass fraction distributions obtained from the numerical simulation are shown in Fig. 5.

Radial water droplet mass fraction distributions obtained from the computational simulation are shown in Fig. 6.

The computational results for the radial distributions are all shown in two graphs with two different ranges of z/D. The reason for this is that the mass fraction values are very large near the nozzle exit (z/D=3-10) and therefore details of the distributions further away from the nozzle cannot be observed.

With the second graph (z/D=20-50) it is possible to analyze the quantitative and qualitative properties of the distributions more explicitly. From these graphs the spread of the jet can be observed. Qualitatively, all radial distributions obtained from the PHOENICS simulations show consistent and physically correct distributions. It is known that the air mass fraction has to increase from a certain value on the centreline to unity at the edge of the jet. Exactly the opposite is valid for the mass fractions of water vapour and water droplets, which have to decrease to zero. Obviously the sum of all the mass fractions has to be one. All these aspects are clearly shown in Figs 4 to 6.

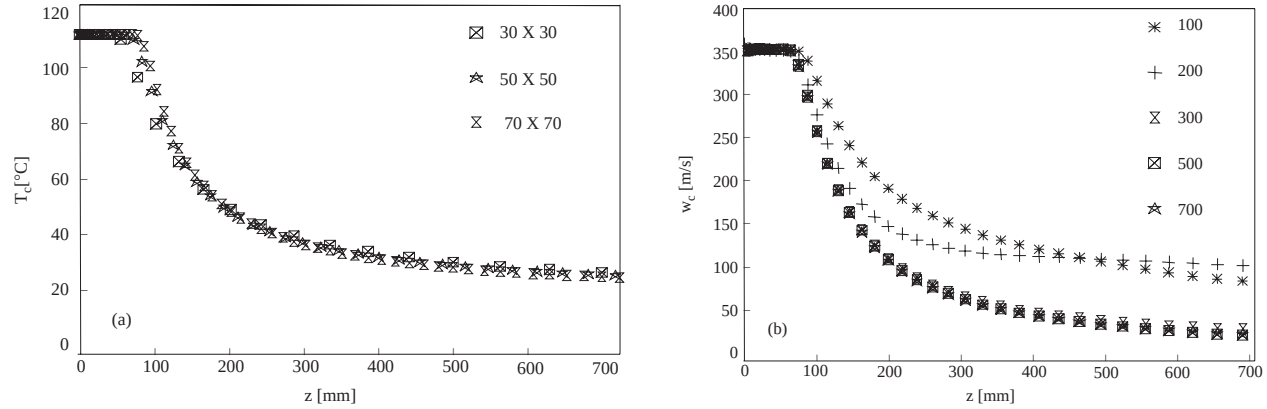

Figure 3. Dependence of the numerical solution on the (a) number of cells and (b) number of sweeps in the axial decay of temperature and velocity, respectively.

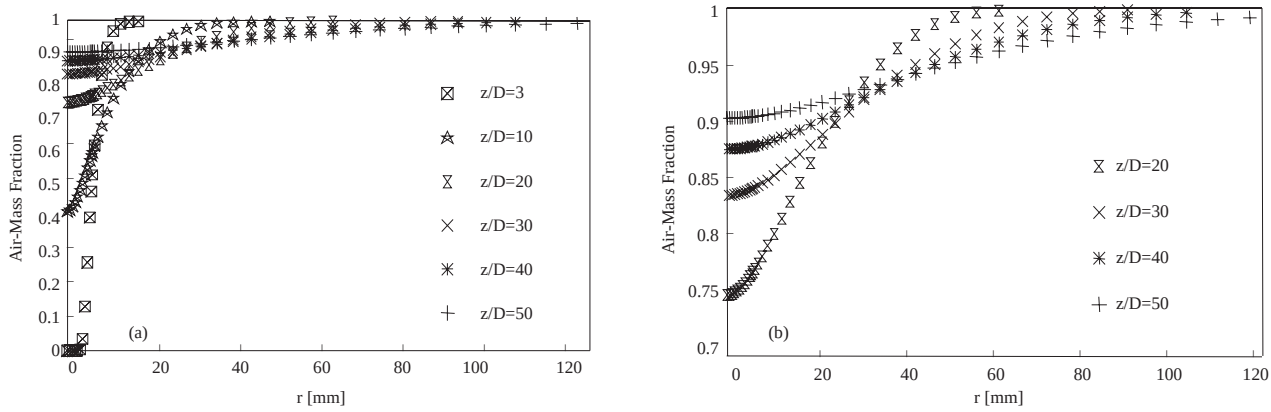

Figure 4. Radial air mass fraction distributions from CFD simulation: (a) z/D=3-50, (b) z/D=20-50

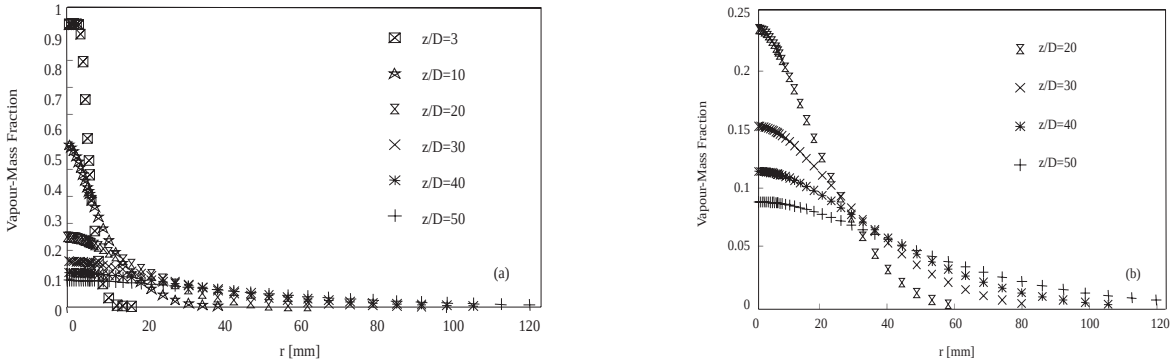

Figure 5. Radial water vapour mass fraction distributions from CFD simulation: (a) z/D=3-50, (b) z/D=20-50

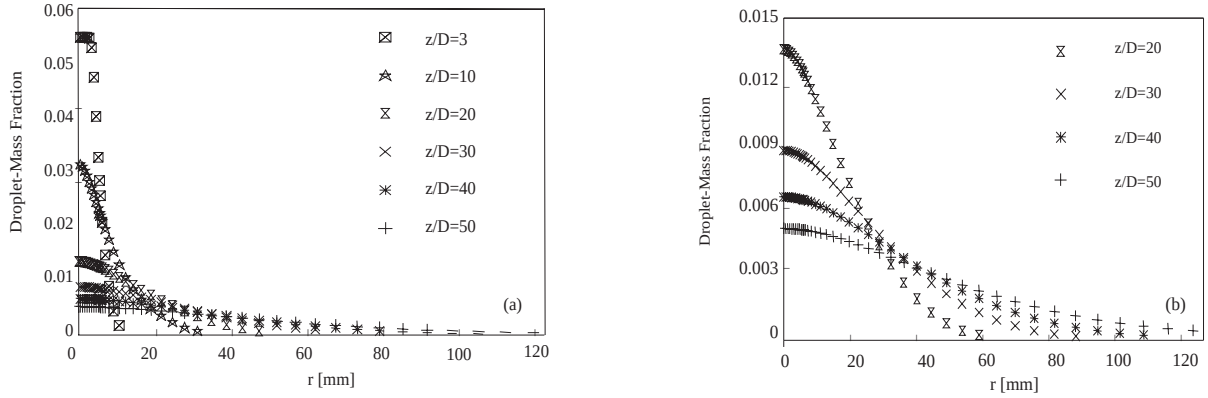

Figure 6. Radial water droplet mass fraction distributions from CFD simulation: (a) z/D=3-50, (b) z/D=20-50

6. Comparison With Experimental Measurements

Radial and centreline distributions of air, water vapour and water droplet mass fractions predicted by PHOENICS are compared with experimental measurements reported by Başkaya et al. (1998).

Fig. 7a compares radial mass fraction distributions of air, water vapour and water droplets from the isokinetic sampling data with results from the predictions at z/D=20, and Fig. 7b compares values at z/D=30. The agreement between isokinetic sampling measurements and numerical simulations is very good, especially at z/D=30.

CFD simulation results for centreline decay of concentration are compared with experimental data in Fig. 8. Starting from the upstream side of the flow, air mass fractions increase in a monotonic manner while steam mass fractions decrease continuously. These variations on the axis of the jet were as anticipated. The mass fraction of air is zero at the nozzle exit, whereas, the mass fraction of steam is one. Hence, mass fraction distributions for air should drop to zero at the edge of the core region, and mass fractions for steam should become one in the core region. The centreline decay of air, water vapour and water droplet mass fractions were quite accurately predicted with the present computational simulation. There are some discrepancies in the vicinity of the transitional region. The reason for this was the high velocities near the nozzle exit which made it impossible to reach the isokinetic sampling condition, hence, no data is available for the near field of the jet (see Başkaya et al., 1998).

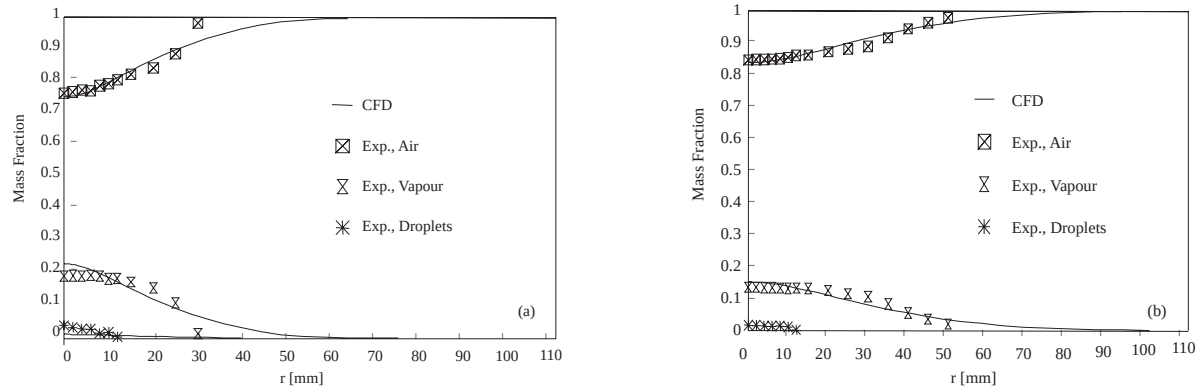

Figure 7. Comparison of CFD results with experimental measurements: (a) z/D=20, (b) z/D=30

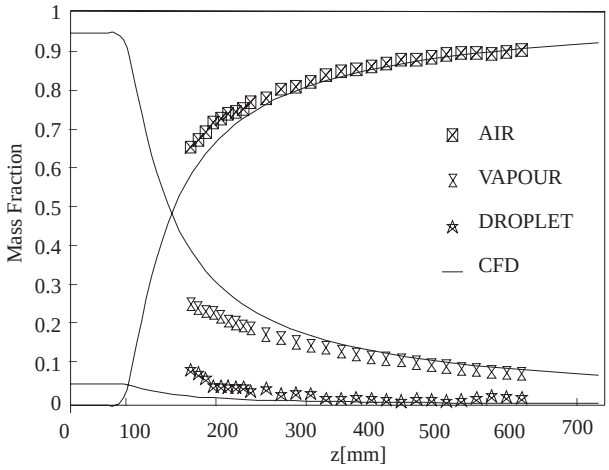

Figure 8. Comparison of centreline decay results between CFD simulation and experimental measurements

The mean concentration along the jet centreline is expected to vary as z^{-1} in self preserving jets. The axial concentration decay law, which can be deduced from similarity considerations, can be expressed as

$$\frac{1}{M_{st}} = C_{DR}\frac{z - z_{O,K}}{r_\varepsilon} \tag{13}$$

where M_{st} is the steam (water vapour + water droplet) mass fraction, C_{DR} is the centreline decay rate, $z_{0,K}$ is the kinematic virtual origin and r_ε is the effective radius. The effective radius concept was introduced by Thring and Newby (1953) as $r_\varepsilon = r_e(\rho_e/\rho_{amb})^{1/2}$ to account for density differences between the jet and ambient fluids. The radius r_ε corresponds physically to the radius of a nozzle for a jet having the same momentum and mass fluxes as the jet under consideration, but with a density ρ_a instead of ρ_e. However, there are reports in the literature (see e.g. Chassaing et al. 1994) that by using the effective radius density effects are reduced but not completely suppressed.

The inverse centreline decay distributions for steam mass fraction are compared in Fig. 9. As can be seen in the graph, the inverse centreline decay from the experiments and CFD simulations are nearly the same. The difference is very small if experimental uncertainties and inaccuracies in the numerical solution procedure are assessed.

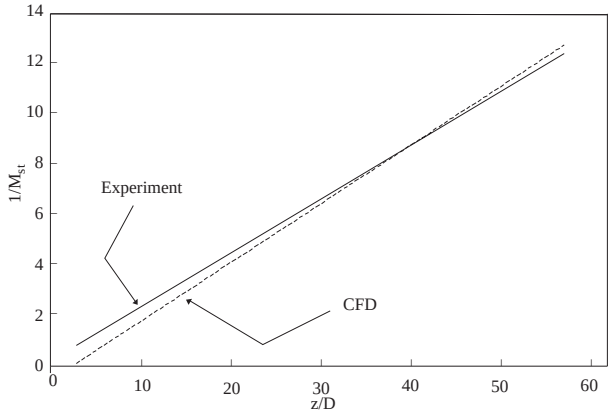

Figure 9. Comparison of inverse centreline decay for steam mass fraction, CFD and experiment.

Table 1. Centreline decay rates reported in the literature compared with present results.

First author, date	Passive scalar	Re	ρ_e/ρ_{amb}	D[mm]	C_{DR}	Range, D
Hinze (1949)	temperature	67000	0.91-1.09	25	0.114	8-40
Becker (1967)	small particles	54000	1.0	6.4	0.0925	20-40
Birch (1978)	methane	16000	0.56	12.6	0.125	20-70
Grandmaison (1982)	small particles	270000	1.0	71.4	0.0923	20-40
Pitts (1991a)	various gases	3950-7890	0.14-5.11	6.4	0.115-0.072	10-35
Richards (1993)	various gases	4000-25000	0.138-1.552	6.4	0.106-0.104	10-60
Başkaya (1998)	water vapour	230000	0.53	12	0.074	<50
Present-CFD	water vapour	230000	0.53	12	0.081	<60

Regression analysis of the data presented in Fig. 9 according to eq. 13 resulted in centreline decay rates of C_{DR}=0.074 for the experimental data and C_{DR}=0.081 for the CFD results. As shown in Table 1 the centreline decay rates from the present investigation are in the range of values reported by other researchers, i.e. 0.072 to 0.125, but slightly smaller than the average value of C_{DR}=0.099 in the literature. So far it has not been explained whether this large scatter in reported values is the result of experimental uncertainties or a breakdown in the similarity assumptions.

7. Conclusions

The numerical simulation results of the axial decay and radial spread of matter for an axisymmetric turbulent steam jet were compared with experimental measurements. The numerical results were in good agreement with experimental data obtained from isokinetic sampling measurements. From this data, centreline decay rates were calculated and compared with data available in the literature. The present results are in the range of values reported in the literature. Hence, the numerical method applied with all its simplifying assumptions can be considered to be adequate enough for the modelling of these steam jets, at least for jets with similar operating conditions. Compared with non-condensing gas jets, concentration distributions were not altered due to condensation as much as temperature distributions, as reported by Başkaya et al. (1997). The outcome of this research project can be used in computational predictions of the environmental effects of steam jet discharges in industrial plants due to pipe breaks.

Acknowledgment

The author would like to thank Dr. A. Gilchrist and Prof. S. M. Fraser of the University of Strathclyde (U.K.) for their discussions and for the computational and experimental facilities provided.

Nomenclature

c_p	Specific heat
C_{DR}	Centreline decay rate
D	Nozzle exit diameter
k	Turbulence kinetic energy
L	Axial length of computational domain
L_c	Characteristic length
m	Mass flow rate
L_c	Characteristic length
m	Mass flow rate
M_{st}	Steam mass fraction
P	Pressure
r	Radial coordinate
r_ε	Effective radius, $r_\varepsilon = r_e(\rho_e/\rho_{amb})^{1/2}$
$r_{1/2}$	Half-width of jet
R	Specific gas constant
R_ρ	Global density ratio, $R_\rho = \rho_e/\rho_{amb}$
R_{eD}	Reynolds number based on D
T	Temperature
w	Axial velocity
z	Axial coordinate
$z_{0,K}$	Kinematic virtual origin

Greek Symbols

α	Mass fraction of air
β	Mass fraction of water vapour
ε	Dissipation rate of turbulence energy
μ	Dynamic viscosity
ρ	Density
ω	Mass fraction of water droplet

Subscripts

air	Air
amb	Ambient
c	Centreline
drop	Water droplet
e	Nozzle exit
mix	Mixture
tot	Total
vap	Water vapour

References

Abramovich, G. N., The Theory of Turbulent Jets, M.I.T. Press Massachusetts, 1963.

Adair, D., Malin, M. R. and Younis, B. A., "Calculations of the Concentration Field of a Turbulent Methane Jet", Appl. Math. Modelling, 16, 476-483, 1992.

Başkaya, Ş., Gilchrist, A. and Fraser, S. M., "Investigation of Axisymmetric Turbulent Steam Jets using Laser-Doppler Anemometry", Proceedings of 6th Intern. Conf. on Laser Anemometry, (ed. Huang, T. T. et al.), Hilton Head, South Carolina, 371-378, 1995.

Başkaya, Ş., Gilchrist, A. and Fraser, S. M., "The Radial Spread and Axial Decay of Temperature in Turbulent Condensing Jets", Int. Comm. Heat and Mass Transfer, 24, 465-474, 1997.

Başkaya, Ş., Gilchrist, A. and Fraser, S. M., "Mixing Characteristics of Turbulent Water Vapour Jets Measured Using an Isokinetic Sampling Probe", Experiments in Fluids, 24, 27-38, 1998.

Becker, H. A., Hottel, H. C. and Williams, G. C., "The Nozzle Fluid Concentration Field of the Round, Turbulent, Free Jet", J. Fluid Mech., 30, 285-303, 1967.

Birch, A. D., Brown, D. R., Dodson, M. G. and Thomas, J. R., "The Turbulent Concentration Field of a Methane Jet", J. Fluid Mech., 88, 431-449, 1978.

Chassaing, P., Harran. G. and Joly, L., "Density Fluctuation Correlations in Free Turbulent Binary Mixing", J. Fluid Mechanics, 279, 239-278, 1994.

Chen, C. J. and Rodi, W., Vertical Turbulent Buoyant Jets, Pergamon Press Oxford, 1980.

Grandmaison, E. W., Rathgeber, D. E. and Becker, H. A., "Some Characteristics of Concentration Fluctuations in Free Turbulent Jets", Can. J. Chem. Eng., 60, 212-219, 1982.

Green, H. G. and Whitelaw, J. H., "Velocity and Concentration Characteristics of the Near-Field of Round Jets", The European Mechanics Colloquium number 237, Marseille, France, 1988.

Hinze, J. O. and van der Hegge Zijnen, B. G., "Transfer of Heat and Matter in the Turbulent Mixing Zone of an Axially Symmetrical Jet", Appl. Sci. Res., A1, 435-461, 1949.

Malin, M. R., "Prediction of Radially Spreading Turbulent Jets", AIAA Journal, 26, 750-752, 1988.

Patankar, S. V., Numerical Heat Transfer and Fluid Flow, Hemisphere, New York, 1980.

Pitts, W. M., "Effects of Global Density Ratio on the Centreline Mixing Behavior of Axisymmetric Turbulent Jets", Experiments in Fluids, 11, 125-134, 1991.

Rajaratnam, N., Turbulent Jets, Developments in Water Science 5, Elsevier, Amsterdam, 1976.

Richards, C. D. and Pitts, W. M., "Global Density Effects on the Self Preservation Behaviour of Turbulent Free Jets", J. Fluid Mech., 254, 417-435, 1993.

Spalding, D. B., The PHOENICS Beginner's Guide, CHAM TR/100, 1991.

Strum, M. L. and Toor, H. L., "Temperature Measurement in Condensing Jets", Ind. Eng. Chem. Res., 31, 706-713, 1992.

Thring, M. W. and Newby, M. P., "Combustion Length of Enclosed Turbulent Jet Flames", Proceedings of 4th Int. Symp. Combust., Pittsburgh, PA, 789-796, 1953.

Vatazhin, A. B., Likhter, V. A. and Shul'gin, V. I., "Turbulent Condensation Jets and the Possibilities of their Control by Means of an Electric Field, Fluid Mechanics-Soviet Research, 14, 10-22, 1985.

Vatazhin, A. B., Valeev, R. S., Likhter, V. A., Shul'gin, V. I. and Yagodkin, V. I., "Investigation of Turbulent Vapour Air Jets in the Presence of Condensation and the Injection of Foreign Particles", Fluid Dynamics, 3, 385-392, 1984.